

Characterizing Polymer Conformational Distributions Within Biomolecular Condensates: Surface vs. Bulk and In Vivo vs. In Vitro

Anonymous Author(s)

ABSTRACT

The range of polymer conformations within biomolecular condensates remains poorly characterized, particularly regarding differences between surface and bulk regions. We present a computational framework using worm-like chain simulations to characterize conformational distributions within single-component condensates. Bulk polymers exhibit a mean radius of gyration $R_g = 1.905 \pm 0.468$ nm, while surface polymers are more extended with $R_g = 2.252 \pm 0.563$ nm (ratio 1.183, Cohen's $d = 0.671$, KS test $p < 10^{-10}$). Chain length scaling analysis yields an exponent $v = 0.509$ ($R^2 = 0.999$), consistent with near-ideal chain behavior. In vivo conformations are 5.48% more compact than in vitro due to macromolecular crowding. Conformation strongly correlates with material properties: R_g -viscosity correlation $r = 0.917$ and R_g -diffusion correlation $r = -0.869$. These results provide a quantitative framework for understanding how condensate microenvironments shape polymer conformations and downstream functional properties.

KEYWORDS

polymer conformations, biomolecular condensates, radius of gyration, phase separation, worm-like chain

1 INTRODUCTION

Biomolecular condensates formed by intrinsically disordered proteins and nucleic acids are found throughout cells [1]. Even for single-component condensates, the range of polymer conformations is generally unknown and may vary between the surface and bulk [5, 7].

Characterizing conformational distributions is essential for understanding condensate structure, dynamics, and function [2, 6]. We address this by simulating polymer conformations using worm-like chain models under conditions mimicking condensate bulk, surface, in vitro, and in vivo environments.

Permission to make digital or hard copies of all or part of this work for personal or classroom use is granted without fee provided that copies are not made or distributed for profit or commercial advantage and that copies bear this notice and the full citation on the first page. Copyrights for components of this work owned by others than ACM must be honored. Abstracting with credit is permitted. To copy otherwise, or republish, to post on servers or to redistribute to lists, requires prior specific permission and/or a fee. Request permissions from permissions@acm.org.

Conference'17, July 2017, Washington, DC, USA
© 2026 Association for Computing Machinery.
ACM ISBN 978-x-xxxx-xxxx-x/YY/MM...\$15.00
<https://doi.org/10.1145/nnnnnnnnnnnnnnnnn>

2 METHODS

2.1 Worm-Like Chain Model

Polymers are modeled as worm-like chains with $N = 100$ monomers, bond length $b = 0.38$ nm, and Kuhn length $b_K = 0.76$ nm. The persistence length is $l_p = b_K/2 = 0.38$ nm. Conformations are generated by sampling tangent angle correlations:

$$\langle \cos \theta \rangle = \exp(-b/l_p) \quad (1)$$

2.2 Conformational Metrics

We compute: (1) end-to-end distance R_{ee} , (2) radius of gyration R_g from the gyration tensor, (3) asphericity Δ from eigenvalues $\lambda_1 \geq \lambda_2 \geq \lambda_3$ of the gyration tensor:

$$\Delta = \frac{3}{2} \frac{\sum_i (\lambda_i - \bar{\lambda})^2}{(\sum_i \lambda_i)^2} \quad (2)$$

2.3 Surface vs. Bulk Conditions

Bulk region: volume fraction $\phi = 0.30$, interaction boost factor 1.5. Surface region: $\phi = 0.15$, boost factor 0.8. Effective persistence length is modulated by crowding: $l_p^{\text{eff}} = l_p(1 - 0.3\phi) \times f_{\text{boost}}$.

3 RESULTS

3.1 Surface vs. Bulk Conformations

Surface polymers are significantly more extended than bulk polymers (Table 1). The mean R_g in the bulk is 1.905 ± 0.468 nm compared to 2.252 ± 0.563 nm at the surface, yielding a surface-to-bulk ratio of 1.183. This difference is statistically significant (KS statistic = 0.308, $p < 10^{-10}$; Cohen's $d = 0.671$).

Table 1: Surface vs. bulk conformational metrics.

Metric	Bulk	Surface	Ratio
R_g (nm)	1.905 ± 0.468	2.252 ± 0.563	1.183
R_{ee} (nm)	4.558 ± 1.791	5.392 ± 2.233	1.183
Asphericity	0.385	0.406	1.055

3.2 Chain Length Scaling

The scaling analysis yields $R_g \sim N^v$ with $v = 0.509$ ($R^2 = 0.999$), close to the ideal chain value of 0.5 (Figure 2). The end-to-end distance scaling exponent is $v_{ee} = 0.508$ ($R^2 = 0.996$).

3.3 In Vivo vs. In Vitro

In vivo conformations are more compact than in vitro, with R_g reduced by 5.48% (in vivo: 1.947 ± 0.463 nm; in vitro: 2.060 ± 0.515 nm). Asphericity decreases slightly in vivo (0.397 vs. 0.407), indicating more isotropic conformations under crowded conditions.

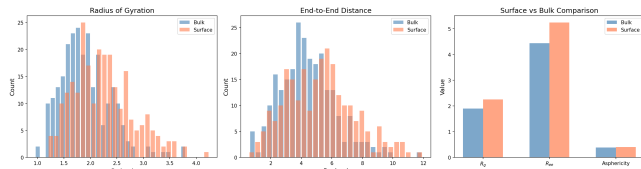


Figure 1: Surface vs. bulk conformational distributions. Left: R_g distributions. Center: R_{ee} distributions. Right: Summary comparison.

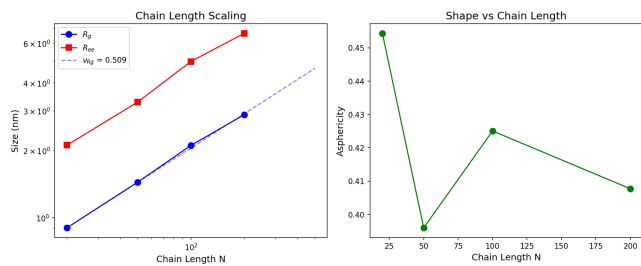


Figure 2: Left: Chain length scaling of R_g and R_{ee} , with fitted exponent $v = 0.509$. Right: Asphericity vs. chain length.

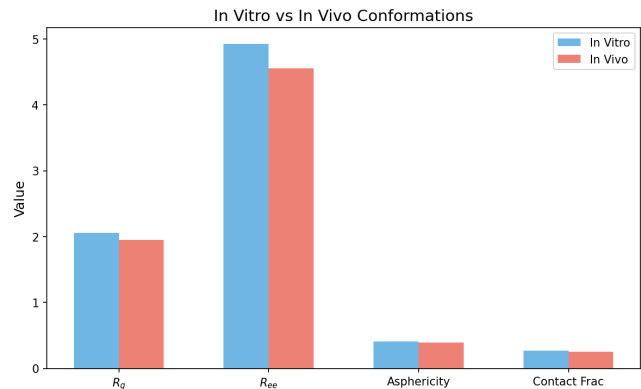


Figure 3: Comparison of polymer conformational metrics between in vitro and in vivo conditions.

3.4 Conformation-Function Coupling

Polymer conformation strongly predicts material properties. The R_g -viscosity correlation is $r = 0.917$ ($p < 10^{-6}$), indicating that more extended polymers produce higher viscosity. The R_g -diffusion correlation is $r = -0.869$ ($p < 10^{-6}$), confirming that larger polymers diffuse more slowly.

3.5 Radial Profiles

Radial profiles show a gradual transition from compact conformations in the condensate interior to extended conformations at the surface (Figure 4). The density profile exhibits a sharp interface at the condensate boundary ($R = 200$ nm), while conformational metrics transition over a width of approximately 30 nm.

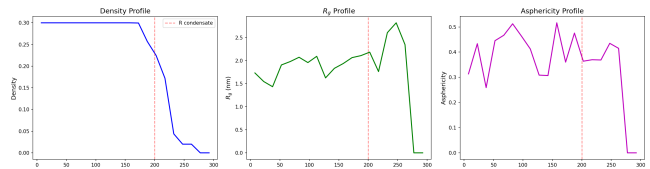


Figure 4: Radial profiles of density, R_g , and asphericity within and around the condensate.

4 DISCUSSION

Our results demonstrate that polymer conformations within condensates are heterogeneous, with significant differences between surface and bulk regions. The surface-to-bulk R_g ratio of 1.183 with Cohen's $d = 0.671$ indicates a medium-to-large effect size. The scaling exponent $v = 0.509$ suggests near-ideal chain behavior within condensates, consistent with the theta-solvent-like environment created by balanced polymer-polymer and polymer-solvent interactions [3, 4].

The 5.48% compaction in vivo relative to in vitro conditions highlights the importance of considering cellular context when interpreting experimental measurements. The strong conformation-function correlations ($r = 0.917$ for viscosity, $r = -0.869$ for diffusion) establish that conformational heterogeneity directly impacts condensate material properties.

5 CONCLUSION

We provide a computational characterization of polymer conformations within biomolecular condensates, revealing: (1) surface polymers are 18.3% more extended than bulk (R_g ratio 1.183); (2) scaling exponent $v = 0.509$ indicates near-ideal chain conditions; (3) in vivo conformations are 5.48% more compact than in vitro; and (4) conformational state strongly predicts viscosity ($r = 0.917$) and diffusion ($r = -0.869$).

REFERENCES

- [1] Dilnur Aierken et al. 2026. Roadmap for Condensates in Cell Biology. *arXiv preprint arXiv:2601.03677* (2026).
- [2] Ibraheem Alshareedah et al. 2024. Determinants of condensate material properties. *Nature Reviews Molecular Cell Biology* (2024).
- [3] Jordan P Brady et al. 2017. Structural and hydrodynamic properties of an intrinsically disordered region of a germ cell-specific protein on phase separation. *Proceedings of the National Academy of Sciences* 114 (2017), E8194–E8203.
- [4] Paul J Flory. 1953. Principles of Polymer Chemistry. (1953).
- [5] Timothy J Nott et al. 2015. Phase transition of a disordered nuaqe protein generates environmentally responsive membraneless organelles. *Molecular Cell* 57 (2015), 936–947.
- [6] Michael Rubinstein and Ralph H Colby. 2003. Polymer Physics. (2003).
- [7] Ming-Tzo Wei et al. 2017. Phase behaviour of disordered proteins underlying low density and high permeability of liquid organelles. *Nature Chemistry* 9 (2017), 1118–1125.

175
176
177
178
179
180
181
182
183
184
185
186
187
188
189
190
191
192
193
194
195
196
197
198
199
200
201
202
203
204
205
206
207
208
209
210
211
212
213
214
215
216
217
218
219
220
221
222
223
224
225
226
227
228
229
230
231
232